Progress In Electromagnetics Research C, Vol. 8, 135–147, 2009

DESIGN OF METALLIC MESH ABSORBERS FOR HIGH BANDWIDTH ELECTROMAGNETIC WAVES

T. Baron, S. Euphrasie, S. Ben Mbarek, P. Vairac and B. Cretin

FEMTO-ST
Université de Franche-Comté, CNRS, ENSMM, UTBM
32 avenue de l'observatoire, F-25044 Besançon Cedex, France

Abstract—In this paper, models of metallic absorbers for electromagnetic waves in the infrared to microwave frequency range are reported and discussed. The Hadley's formalism (1D model) of transmission, reflection and absorption for semi-infinite layers, which allows to design all configurations of unstructured absorber films and dielectrics is generalized. To make the micro-fabrication of the metallic absorbers easier (that means to have layers thick enough), the metallic layers need to be structured (grid for example). We developed a model that allows us to consider the structure of metal as a homogeneous layer, where the diffraction is negligible. This new layer can be used with the previous model. When diffraction effects must be taken into account, we modified an electrical model made by Ulrich. We further developed it for the configuration of a dielectric before the metallic grid. The results showed the importance to take into account all the dimensions of the grid, the dielectric layer parameters and the wavelength to design the best absorber.

1. INTRODUCTION

One way to detect electromagnetic waves in the infrared to microwave frequency range is to use a bolometer. This sensor converts the energy of an electromagnetic wave to heat, which is then transformed to an electrical signal. Bolometers are made of two main parts: An absorber and a thermal sensor. The absorber converts the incident wave into thermal energy by ohmic effect. Metal films can be used as absorbers for infrared and millimeter-wave radiations [1–3]. The best absorption

Corresponding author: T. Baron (thomas.baron@femto-st.fr).

properties are however obtained for very thin metal films, e.g., of the order of a few nanometer, which is generally difficult to achieve, from a fabrication point of view. A solution initially proposed by Bock et al. is to structure the otherwise homogeneous metal film [6]. By way of explanation, they quote the work of Ulrich [5]. However, this study concerned the filters and not the absorbers. This method has then been experimentally implemented [7, 8], but the design of the absorber usually relies on empirical experimentations.

The conception of such structured absorbers is usually based on empirical experimentations. The aim of this paper is to propose a model of such structured metallic absorbers that allows to understand the phenomena and can be used to facilitate their design.

2. SUPPORTED METAL FILM

Several models exist to calculate the absorption, transmission and reflection of a plane-wave through homogeneous semi-infinite media.

Hadley and Dennison [1] presented a formalism for a single metallic layer and for interference filters constituted by metal-dielectric-metal layers, for which the thickness of the second metal is the same as the first one for transmission filters or thick enough to act as a mirror for reflection filters. In the case of unsupported metallic films, they showed that the maximum absorption is 50% of the incident power.

Hilsum [2] simplified the absorption's formulation in the case of normal incidence. For unsupported film, the power absorption, A_H, is then:

$$A_H = \frac{4f}{(f+2)^2} \tag{1}$$

In this formulation, f is the ratio of free space impedance to the resistance per square of the film. It was defined as $Z_0 \sigma s$, where σ and s are, respectively, the conductivity and thickness of the metal. The impedance of vacuum is noted Z_0 and is equal to $377\,\Omega$. Since an unsupported metal film in air is difficult to fabricate, Hilsum [2] considered the addition of a dielectric substrate with or without another metal film with the same thickness as the first one. He showed that the dielectric film allows to obtain an absorption of at least 70%.

Silberg [3] reported a generalization of Hilsum's problem with the second metallic film exhibiting an arbitrary thickness. Thus, absorption rates greater than 95% could be obtained.

The analytical solutions obtained by these models allow to calculate the best thickness of the different layers. We will now propose a generalization for all the possible configurations.

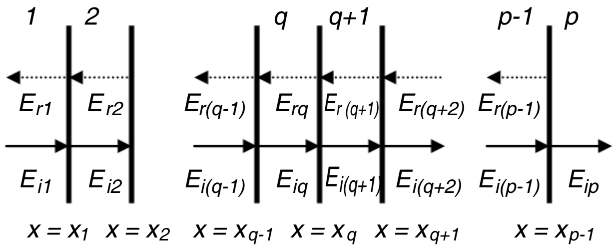

Figure 1. Representation and notation used for specifying the p media and incident, reflected, and transmitted waves.

Let us consider the one dimensional system with p media as shown in Figure 1, using the same formalism as previously.

The system is in air, therefore the first and last media have a refractive index $n_1 = n_p$ equals to unity. The considered media can be dielectrics with a refractive index n_q or metal films with a conductivity σ_q, an index of refraction η_q and an extinction coefficient κ_q, with the approximation:

$$\eta_q = \kappa_q = \sqrt{\frac{\sigma_q}{2\omega\epsilon_0}} \tag{2}$$

with ω the pulsation of the wave. The propagation constant k_q noted k_{qd} in the case of a lossless dielectric and k_{qm} for metallic media:

$$k_{qd} = \frac{2\pi n_q}{\lambda} \tag{3}$$

$$k_{qm} = \frac{2\pi\left(\eta_q + j\kappa_q\right)}{\lambda} \tag{4}$$

with λ the wavelength in vacuum. The interface between two media q and $q+1$ is at the abscissa $x = x_q$. This abscissa is taken as the phase reference of the propagating (incident and reflected) waves in the medium number $q+1$. The first medium is an exception since its phase reference is $x = x_1$.

Like Hadley [1], we suppose the continuity of tangential electrical and magnetic fields. For the electrical field, it is always true. For the magnetic field, it is true only when volume currents are considered without surface currents. In the case of the system represented in Figure 1, the boundary conditions at the interface $x = x_q$ are, for normal incidence:

$$E_{iq}e^{jk_qx} + E_{rq}e^{-jk_qx} = E_{i(q+1)} + E_{r(q+1)} \tag{5}$$

$$E_{iq}e^{jk_qx} - E_{rq}e^{-jk_qx} = \frac{n_{q+1}}{n_q}\left(E_{i(q+1)} - E_{r(q+1)}\right) \tag{6}$$

Therefore, we obtain:

$$E_{iq} = \frac{e^{-jk_q t_q}}{2}\left[\left(1+\frac{n_{q+1}}{n_q}\right)E_{i(q+1)} + \left(1-\frac{n_{q+1}}{n_q}\right)E_{r(q+1)}\right] \quad (7)$$

$$E_{rq} = \frac{e^{jk_q t_q}}{2}\left[\left(1-\frac{n_{q+1}}{n_q}\right)E_{i(q+1)} + \left(1+\frac{n_{q+1}}{n_q}\right)E_{r(q+1)}\right] \quad (8)$$

with $t_q = x_q - x_{q-1}$.

The power transmission coefficient T is given by $E_{ip}E_{ip}^*/E_{i1}E_{i1}^*$, the power reflection coefficient R by $E_{r1}E_{r1}^*/E_{i1}E_{i1}^*$, and the power absorption coefficient A by $1 - R - T$.

By taking E_{ip} equals to unity, the series defined by Equations (7) and (8) allow to calculate E_{i1} and E_{r1}, then T, R and A. This method allows the prediction of the absorption, transmission and reflection for all the configurations with the assuming infinitely plane layers and with normal incident waves (these equations can be easily modified in non-normal incidence but will not be discussed here).

As predicted by the analytical solutions for the simple cases described above, an unsupported metallic film absorber should have a surface impedance of $188.5\,\Omega$ to allow for the greatest absorption. The thickness of such a film would be very small. For instance, with a resistivity $\rho = 54\,\mu\Omega\cdot$ cm, the thickness is less than 3 nm. Furthermore, the maximum power absorption coefficient is 50%. By adding of a dielectric film, it is possible to have 85% of absorption with a thicker metallic film. But again remember that the manufacturing process of these metal films is difficult. A possibility to overcome this problem is to use a structured metal absorber.

3. ABSORPTION OF STRUCTURED METAL LAYERS

The absorbers previously described are hardly feasible due to their thickness. Several authors [6–8] overcame this problem by structuring their metallic absorbers. Bock et al. [6] based their conception on Ulrich's models [5]. Ulrich studied grids for filter applications: Transmissive grids are called capacitive grids, and reflective grids are called inductive grids. These names were chosen since he used equivalent inductive and capacitive electrical circuit representations where the different parameters were fitted to his measures.

The inductive grids are presented in Figure 2(a). According to Ulrich the electrical field is continuous across the grids, and the profile of the current, localized in the skin depth in both sides of the metal, is symmetric.

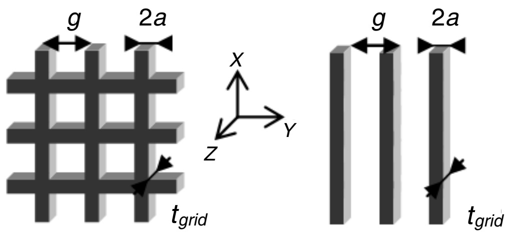

(a) (b)

Figure 2. (a) Inductive grid; (b) inductive line (linearly polarized wave along the X direction).

Contrary to Ulrich, we used an asymetric current profile, which follows an exponential decrease across the grid. This exponential decrease is governed by the equivalent skin depth parameter δ_{eq}, which is different from the intrinsic skin depth of the metal δ. It also depends on the metal conductivity σ and on the geometry of the grid. We will initially assume that the pitch g is very small compared to wavelength λ and that the grid is placed in free space. We also consider a linearly polarized wave along the vertical lines of the grid that is to say along the X direction. Since $g \ll \lambda$, diffraction effects are neglected. This system has a complex reflective coefficient of the electrical field Γ and a complex transmission coefficient Λ.

3.1. Absorption of Inductive Lines

First, we will consider the inductive line geometry, presented in Figure 2(b). For the sake of simplicity, we suppose a progressive plane wave with no reflection on the second interface. The absorption is due to the current in the metallic structure by Joule effect. The volume density current J_x (along the X direction) has an exponential decrease as supposed before:

$$J_x = \sigma E = J_0 e^{\frac{-z}{\delta_{eq}}} e^{\frac{-jz}{\delta_{eq}}} e^{-j\omega\tau} \tag{9}$$

with τ the time and z the position, with $z = 0$ corresponding to the first interface.

The difference of the magnetic fields H_y on the two interfaces of the metallic structure ($z = 0$ and $z = t_{grid}$) is proportional to the incident magnetic field H_i. Furthermore, it depends on the complex reflective coefficient Γ (for the electrical field, -Γ for the magnetic field) and on the complex transmission coefficient Λ of the system. This difference is due to the volume density current J_x as predicted by Maxwell-Ampere law:

$$H_y(t_{grid}) - H_y(0) = (\Lambda - (1-\Gamma))H_i = -\frac{1}{\eta}\int_0^{t_{grid}} J_x dz \tag{10}$$

η is a dimensionless form-factor equal to $g/2a$. If we consider the approximation $\Lambda = 1 + \Gamma$ (continuity of the electrical tangential field, which can be used when the metal thickness is much smaller than the equivalent skin depth, which will be introduced later).

$$2\Gamma H_i = -\frac{1}{\eta}\int_0^{t_{grid}} j_x dz \tag{11}$$

With the Equations (9) and (11), we can easily determine the current density J_0.

$$J_0 = \frac{2\Gamma H_{il}\eta(1+j)}{\delta_{eq}\left(e^{\frac{-(1+j)t_{grid}}{\delta_{eq}}} - 1\right)} \tag{12}$$

From Equations (9) and (12), the surface dissipated power by Joule effect P_d is:

$$P_d = \frac{1}{g^2}\overline{\iiint \frac{1}{\sigma}\Re(J_x)^2 dV}^{\tau} = \frac{\delta_{eq}}{4\sigma\eta}\left|J_0\right|^2\left[1 - e^{\frac{-2t_{grid}}{\delta_{eq}}}\right] \tag{13}$$

$\Re(J_x)$ is the real part of J_x, $\overline{}^{\tau}$ corresponds to the time average.

The absorption A is the ratio of dissipated P_d to incidence P_i surface power.

$$A = \frac{\frac{4\eta}{\delta_{eq}\sigma}\frac{|\Gamma|^2}{Z_0}\left[1 - e^{\frac{-2t_{grid}}{\delta_{eq}}}\right]}{1 + e^{\frac{-2t_{grid}}{\delta_{eq}}} - 2e^{\frac{-t_{grid}}{\delta_{eq}}}\cos\left(\frac{t_{grid}}{\delta_{eq}}\right)} \tag{14}$$

We consider an equivalent homogeneous material of the inductive line, characterized by an equivalent conductivity.

$$\sigma_{eq} = \frac{\sigma}{\eta} \tag{15}$$

The equivalent skin depth of this equivalent homogeneous material is:

$$\delta_{eq} = \sqrt{\frac{2}{\omega\sigma_{eq}\mu}} \tag{16}$$

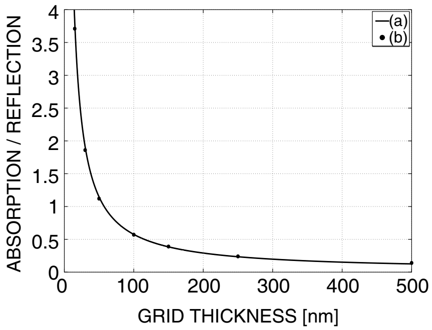

Figure 3. Comparison of the ratio absorption to reflection as a function of the grid thickness (a) analytical results from our model and (b) 2-dimensional numerical results obtained with COMSOL MULTIPHYSICS software for an inductive line characterized by $\lambda/g = 10$ and $\eta = 10$.

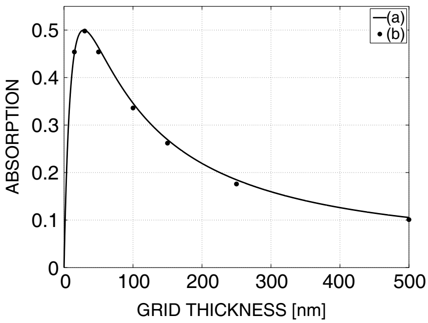

Figure 4. Comparison for unsupported metal between (a) analytical results come from our developed model for a metallic film with an equivalent conductivity $\sigma_{eq} = \sigma/\eta$ and (b) 2-dimensional numerical results obtained with COMSOL MULTIPHYSICS software for an inductive line characterized by λ/g and η. Numerical values: $\lambda/g = 100$, $\eta = 10$ and $\sigma = 1851851\ \Omega^{-1}\cdot\text{m}^{-1}$.

With titanium's bulk characteristic, the equivalent skin depth parameter δ_{eq} equals 676.7 nm when η is 10. Note that the intrinsic skin depth of the metal δ is 214 nm.

To validate this model, numerical simulations using COMSOL MULTIPHYSICS RF module were performed in two dimensions. Boundary conditions were used to have a plane-wave. λ was taken equal to one hundred micrometers. Different ratios λ/g and $g/2a$ were taken as parameters and the thickness t_{grid} of the grid as the variable. We used titanium with its bulk characteristics. Figure 3 shows a comparison between our model (Equation (14)) and the simulation results. Model and simulations are in complete agreement.

This equivalent homogeneous material can be used in the configuration of the previous paragraph. In this case, the thickness of this equivalent homogeneous material is multiplied by the $g/2a$ ratio to have the same absorption as for the metallic film. Figure 4 shows the comparison between our model (Equation (16) combined with our algorithm presented in paragraph II) and the simulation results.

Our model is therefore validated by simulation results. This model is all the better as g/λ is the more negligible. This model remains valid as long as g/λ ratio is smaller than 0.1. Above this value, it overestimates absorption with an error of 4% compared to the simulations. Furthermore, in the particular case of η close to unity, we find the results predicted for homogeneous metal films.

Note that contrary to Ulrich, the thickness of the metal is important. The main reason is that Ulrich used very thick grids.

Our model allows for the conception of the inductive lines with small errors if the ratio g/λ is small. In order to be able to consider any (arbitrary) polarizations, grids are used instead of lines.

3.2. Inductive Grid Absorption

We now consider the inductive grid, presented in Figure 2(a). We realize this study in the same conditions as for the inductive line with the same hypothesis. For an elementary crossed line in the Y direction, we suppose that the current density J_z in the metal is described in Equation (17).

$$J_z = J_0 \sin\left(2\pi\left(\frac{x_s + a}{\lambda}\right)\right) \tag{17}$$

x_s corresponds to the position in the horizontal line numbered s, with x_s between $-a$ and a.

The dissipated power P_d is now the sum of P_{d1} and P_{d2}, with P_{d1} the dissipated power in the vertical line and P_{d2} the dissipated power in the rest of the structure (horizontal line). P_{d1} corresponds to the dissipated power described in the last paragraph for inductive line.

The same type of calculation as before leads to an equivalent homogeneous material with the conductivity σ_{eq} given by Equation (18).

$$\sigma_{eq} = \sigma\left[\frac{2a}{g} + \frac{g-2a}{g^2}\left(a - \lambda\frac{\sin(4\pi a/\lambda)}{4\pi}\right)\right] \tag{18}$$

Note that P_{d2} is usually far smaller than P_{d1}.

With this equivalent media, we can determine the optimum thickness of the grid to have the highest absorption with the one-dimension model presented before. It is now possible to design unsupported grid with a dielectric layer to increase absorption.

4. ELECTRICAL MODEL

Our model allows for the design of grids with ratios g/λ smaller than 0.01 with negligible errors. However, technology limits g/λ and $g/2a$ ratios. Therefore diffraction effects must be taken into account.

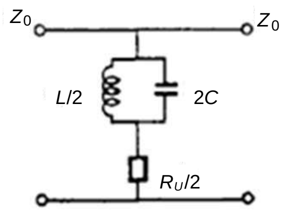

Figure 5. Equivalent circuit for thin inductive grids given by Ulrich [5].

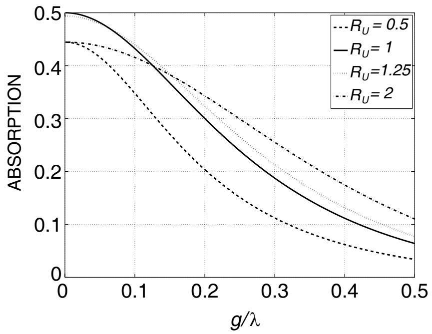

Figure 6. Influence of impedance of the grid.

Furthermore, the grids are usually supported by dielectric, which also must be included.

4.1. Unsupported Grids

To take into account the diffraction effects, R. Ulrich used an electrical analogy based on his experiments [5], shown in Figure 5. R_U represents ohmic losses to take into account the grid absorption. R. Ulrich has shown that Marcuvitz's formula [9] for L and C gives a good fit for ratios a/g smaller than 15%.

The absorption A_U of this equivalent electrical circuit is given by Equation (19).

$$A_U = 2R_U \left|\Gamma\right|^2 = \frac{2R_U}{\left(1+R_U\right)^2 + \left(L\omega/(1-LC\omega^2)\right)^2} \tag{19}$$

The first metallic grid, which was designed for absorbing the infrared radiation was presented in 1995 [6]. This grid was suspended on air by supporting legs. The authors used Ulrich's model with $R_U = 1$ (corresponding to a surface impedance of $188.5\,\Omega$ for a film) and showed the influence of the $g/2a$ ratio of the grid for different g/λ ratio: Absorption increased with the $2a/g$ ratio.

Due to technology limits the ratio g/λ is limited, so the conception of the grid must take into account the ratio g/λ. Figure 6 presents the absorption of a suspended grid on air with a $2a/g$ ratio of 5% for different R_U. The best configuration of thickness for a given geometry (g, $2a$) directly depends on the g/λ ratio.

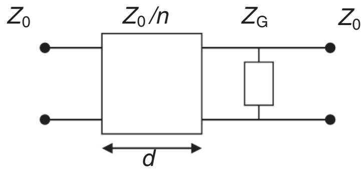

Figure 7. Equivalent circuit for a grid (impedance Z_G) supported by a dielectric (characteristic impedance Z_0/n, length d, and refractive index n).

Thus, we can find, for a given ratio g/λ (the one chosen for technology's sake), the optimum R_U of the grid. In other words, it is possible to have an optimum thickness t_{grid} for particular g/λ and $g/2a$ ratios.

4.2. Grids with a Dielectric Layer

Practically, the grids are usually supported by a dielectric substrate. Let us therefore consider Figure 7. The line representing the dielectric has a characteristic impedance $Z_n = Z_0/n$ and a length d. Its propagation coefficient is $\beta = 2\pi n/\lambda$. The grid is modelled as a lumped impedance Z_G, as shown before in Figure 5. The rest of the line has a characteristic impedance Z_0.

Since there is no reflection after the grid, the rest of the line can be replaced by a discrete element of impedance Z_0. In the electrical transmission line model, we can calculate the equivalent impedance Z_T of the system: The dielectric line and the two parallel discrete impedances Z_0 and Z_G seen in the plane just before the line representing the dielectric. The reflective coefficient in voltage before the dielectric Γ is given by Equation (20).

$$\Gamma = \frac{Z_T/Z_0 - 1}{Z_T/Z_0 + 1} \tag{20}$$

The transmission coefficient Λ is given by Equation (21) obtained from the calculation of the electrical line output current.

$$\Lambda = \frac{4}{\left|\cos(\beta d)\left[\frac{Z_0}{Z_G} + 2\right] + j\sin(\beta d)\left[\frac{1}{n}(\frac{Z_0}{Z_G} + 1) + n\right]\right|^2} \tag{21}$$

The absorption coefficient A is given by Equation (22) obtained from the calculation of the current in ohmic resistance R of the model of the grid.

$$A = \frac{2R}{\left|\cos(\beta d)\left[2\frac{Z_G}{Z_0}+1\right] + j\sin(\beta d)\left[\frac{1}{n}(\frac{Z_G}{Z_0}+1)+n\frac{Z_G}{Z_0}\right]\right|^2} \tag{22}$$

with Z_G the impedance of the grid:

$$Z_G = Z_0\left[\frac{R}{2} - j\frac{1}{2}\frac{L\omega}{1-LC\omega^2}\right] \tag{23}$$

The normalized ohmic resistor R, which characterizes the ohmic losses is given by Equation (24). We replace R_U by R in the Ulrich's equivalent electrical model of the metallic grid to explicit our relation with metallic grid parameters. The normalized ohmic resistor R is obtained from Equation (14) and from the relation $A = 2R\,|\Gamma|^2$ in the case of metallic grid alone.

$$R = \frac{\frac{2\eta}{\delta_{eq}\sigma}\frac{1}{Z_0}\left[1 - e^{\frac{-2t_{grid}}{\delta_{eq}}}\right]}{1 + e^{\frac{-2t_{grid}}{\delta_{eq}}} - 2e^{\frac{-t_{grid}}{\delta_{eq}}}\cos\left(\frac{t_{grid}}{\delta_{eq}}\right)} \tag{24}$$

Results obtained with our first model (without diffraction effects) and with this latter model in the case of $2a/g$ equals to 0.1 and g/λ equals to 0.01 are the same. With increasing g/λ, they differ since diffraction effects are taken into account in the second model.

Figure 8 shows the influence of the dielectric thickness on the absorption. The two curves show that the best thickness to have the highest absorption is no longer a quarter of the wavelength because of diffraction effects. For instance, with $g/\lambda = 0.2$, the best absorption is obtained for a dielectric thickness is 95% of this value. The optimum thickness must therefore be calculated using all the parameters $(t_{grid}, \lambda, g, a)$.

Figure 9 shows the absorption versus the wavelength λ of a grid with a dielectric optimized for a wavelength of 100 µm. The parameters a and g, respectively, equal 3 µm and 20 µm. The absorption is optimized only for a band of frequency. This is partially because of the dielectric, which can reduce the absorption instead of to increase it, if it is used at frequencies different from those for which it was designed. In that case, absorbers have a finite bandwidth.

Although Ulrich's expression is relevant in many situations, we suggest that in the future the expression given here will be used instead. With this model, it is possible to find easily the optimum parameters to have the best absorption.

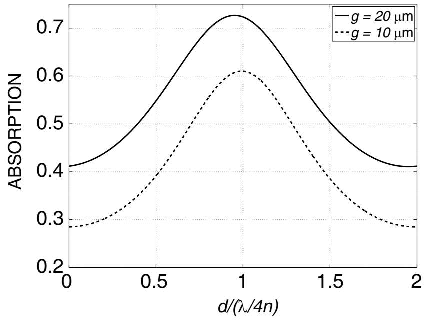

Figure 8. Absorption of 23 nm thick titanium grids with a resistivity of 54 μΩ·cm as a function of the dielectric's thickness. $g = 20\,\mu\text{m}$ and $g = 10\,\mu\text{m}$ with $a = 3\,\mu\text{m}$ and dielectric coefficient of 2.9.

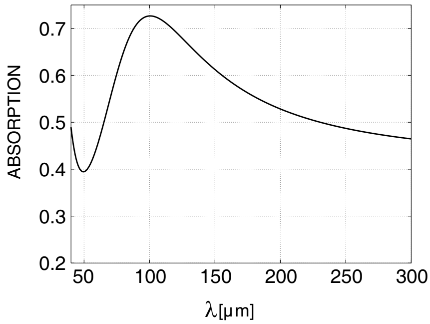

Figure 9. Absorption of 23 nm thick titanium grids with a resistivity of 54 μΩ·cm as a function of the wavelength λ. $a = 3\,\mu\text{m}$, $g = 20\,\mu\text{m}$ and $d = 0.95\lambda/4n$ with dielectric coefficient of 2.9.

5. CONCLUSIONS AND PERSPECTIVES

A bolometer is a sensor based on the absorption of electromagnetic waves. In order to design a bolometer, the theory of the absorption of metallic structures was studied. The simple model of semi-infinite layers has already shown the best configuration with one metallic layer (surface impedance of 188.5 Ω). The generalization of this model allowed to choose other configurations for the absorber with more metal or dielectric layers. However, the obtained metallic thickness is usually too small to be easily fabricated using standard microfabrication techniques. One solution is to structure the metallic layer. Until now, theory of such structures was studied only for filter applications where the absorption rate is small. We modified Ulrich's theory for unsupported metallic grids. It still showed the dependence of the metallic structures absorption with the wavelength. In this context, the best design is not necessary the same for different wavelengths. Furthermore, an equivalent metallic homogeneous model was implemented to simplify the conception. Using the semi-infinite model, the best configuration with only one metal layer is to have the dielectric before the metal layer. We have adapted the electrical model for this configuration. The results show that the optimum dielectric thickness to have the best absorption changes according to the structuration of the grid. This model shows the necessity to take into account all the dimensions of the absorbers to design the optimized structures.

ACKNOWLEDGMENT

The authors thank the French ANR program for supporting this project.

REFERENCES

1. Hadley, L. N. and D. M. Dennison, "Reflection and transmission interference filters," *J. Opt. Soc. Am.*, Vol. 37, 451–465, 1947.
2. Hilsum, C., "Infrared absorption of thin metal films," *J. Opt. Soc. Am.*, Vol. 44, 188, 1954.
3. Silberg, P. A., "Infrared absorption of three-layer films," *J. Opt. Soc. Am.*, Vol. 47, 575–578, 1957.
4. Mahan, G. D. and D. T. F. Marple, "Infrared absorption of thin metal films: Pt on Si," *Appl. Phys. Lett.*, Vol. 42, No. 3, 219–221, Feb. 1983.
5. Ulrich, R., "Far-infrared properties of metallic mesh and its complementary structure," *Infrared Physics*, Vol. 7, 37–55, 1967.
6. Bock, J. J., D. Chen, P. D. Mauskopf, and A. E. Lange, "A novel bolometer for infrared and millimeter-wave astrophysics," *Space Science Reviews*, Vol. 74, 229–235, 1995.
7. Mauskopf, P. D., J. J. Bock, H. D. Castillo, W. L. Holzapfel, and A. E. Lange, "Composite infrared bolometers with Si3N4 micromesh absorbers," *Applied Optics*, Vol. 36, No. 4, 765–771, 1997.
8. Griffin, M. J., "Bolometers for far-infrared and submillimetre astronomy," *Nuclear Instruments and Methods in Physics Research*, Sect. A, Vol. 444, 397–403, 2000.
9. Marcuvitz, N., *Waveguide Handebook*, M.I.T. Rad. Lab. Ser., McGraw-Hill, 1951.